XIII International Conference on Computational Plasticity. Fundamentals and Applications
COMPLAS XIII
E. Oñate, D.R.J. Owen, D. Peric and M. Chiumenti (Eds)

A NUMERICAL METHOD FOR CALCULATING THE STRAIN RATE INTENSITY FACTOR

SERGEI ALEXANDROV[*] AND CHIHYU KUO[†]

[*] Institute for Problems in Mechanics
Russian Academy of Sciences
101-1 Prospect Vernadskogo, 119526 Moscow, Russia
e-mail: sergei_alexandrov@spartak.ru, www.ipmnet.ru

[†] Division of Mechanics, Research Center for Applied Sciences
Academia Sinica,
128, Sec.2, Academia Road, 115 Taipei, Taiwan
email: cykuo06@gate.sinica.edu.tw, www.rcas.sinica.edu.tw

Key words: Perfectly plastic solids, Friction, Singularity, Strain rate intensity factor.

Abstract. The strain rate intensity factor is the coefficient of the leading singular term in a series expansion of the equivalent strain rate in the vicinity of maximum friction surfaces. In the case of rigid perfectly plastic solids, the maximum friction law postulates that the friction stress at sliding is equal to the shear yield stress. The equivalent strain rate approaches infinity near maximum friction surfaces. Therefore, the strain rate intensity factor cannot be calculated by means of standard finite element packages. On the other hand, the strain rate intensity factor can be used to predict the generation of fine grain layers in the vicinity of friction surfaces in metal forming processes. In order to develop a model that connects the strain rate intensity factor and parameters characterizing such layers, it is necessary to propose a numerical method for calculating the strain rate intensity factor with a high accuracy. In the present paper, the strain rate intensity factor is expressed in terms of quantities that are found by means of conventional numerical methods based on the theory of characteristics. Then, an available numerical method is complemented with an additional procedure to find the strain rate intensity factor. The new method is used to calculate the strain rate intensity factor in compression of a plastic layer between parallel plates. The approach proposed is restricted to plane strain deformation of rigid perfectly plastic material.

1 INTRODUCTION

The strain rate intensity factor has been introduced in [1] as the coefficient of the leading term in a series expansion of the equivalent strain rate in the vicinity of maximum friction surfaces. The leading term of this expansion follows an inverse square root rule near maximum friction surfaces. Hence the equivalent strain rate approaches infinity in the vicinity of such surfaces. For this reason standard commercial finite element packages are not capable to calculate the strain rate intensity factor. On the other hand, the maximum friction law is often accepted as a boundary condition to describe metal forming and cutting processes [2 -

13]. In real processes and special purpose experiments, a layer with drastically modified material properties is generated in the vicinity of surfaces with high friction [2 – 13]. This is in qualitative agreement with the main result obtained in [1] since many material properties are affected by the equivalent strain rate and the strain rate intensity factor controls the magnitude the equivalent strain rate in the vicinity of maximum friction surfaces. Moreover, the expansion found in [1] predicts a very high gradient of the equivalent strain rate near maximum friction surfaces. An approach to connect the strain rate intensity factor and the distribution of material properties in a narrow layer near surfaces with high friction has been proposed in [14]. In order to apply this approach, it is necessary to develop a numerical method to calculate the strain rate intensity factor with a high accuracy. Such a method is proposed in the present paper for plane strain deformation of rigid perfectly plastic material. The method is based on the method of characteristics. The numerical method is adopted to find the distribution of the strain rate intensity factor in compression of a plastic layer between rigid parallel plates. It is shown that the distribution of the strain rate intensity factor is given by a discontinuous function. Comparison with Prandtl's cycloid solution is made.

In addition to rigid perfectly plastic material considered in [1], the strain rate intensity factor has been introduced for more general material models in [15 – 17].

2 STRAIN RATE INTENSITY FACTOR IN CHARACTERISTIC COORDINATES

In the case of rigid perfectly plastic materials the maximum friction surface is defined by the condition that the friction stress at sliding is equal to the shear yield stress, $k = constant$. The equivalent strain rate in the vicinity of maximum friction surfaces is represented as [1]:

$$\xi_{eq} = \frac{D}{\sqrt{s}} + o\left(\frac{1}{\sqrt{s}}\right) \tag{1}$$

as $s \to 0$. Here s is the normal distance to the maximum friction surface and D is the strain rate intensity factor. In the case of plane strain deformation the equivalent strain rate is given by:

$$\xi_{eq} = \sqrt{\frac{2}{3}}\sqrt{\xi_{q_1q_1}^2 + \xi_{q_2q_2}^2 + 2\xi_{q_1q_2}^2}\,. \tag{2}$$

Here $\xi_{q_1q_1}$, $\xi_{q_2q_2}$ and $\xi_{q_1q_2}$ are the components of the strain rate tensor in an arbitrary ortogonal curvilinear coordinate system (q_1, q_2). It is known that planar flow of rigid perfectly plastic material is described by a hyperbolic system of equations [18]. Let the two families of characteristics be labeled by the parameters α and β. Then [18],

$$\phi = \alpha + \beta \tag{3}$$

and

$$\frac{1}{R} = \frac{\partial \phi}{\partial s_\alpha}, \quad \frac{1}{S} = -\frac{\partial \phi}{\partial s_\beta} \tag{4}$$

where ϕ is the anti-clockwise angular rotation of the $\alpha-$ line from any fixed direction, $\partial/\partial s_\alpha$ and $\partial/\partial s_\beta$ are space derivatives taken along the $\alpha-$ and $\beta-$ lines, respectively, R is

the radius of curvature of the $\alpha-$ lines, and S is the radius of curvature of the $\beta-$ lines. The $\alpha-$ and $\beta-$ lines can be regarded as a pair of right – handed curvilinear ortogonal coordinates. The orientation of these lines is chosen such that the algebraically greatest principal stress σ_1 falls in the first and third quadrants. The angle between the direction of this stress and each of the characteristic directions is $\pi/4$ (Figure 1). The normal strain rates vanish in the characteristic coordinates [18]. Therefore, equaton (2) in which $q_1 \equiv \alpha$ and $q_2 \equiv \beta$ becomes:

$$\xi_{eq} = \frac{2}{\sqrt{3}}\left|\xi_{\alpha\beta}\right| \tag{5}$$

where $\xi_{\alpha\beta}$ is the shear strain rate in the characteristic coordinates. Introduce a Cartesian coordinate system (x, y). The angle ϕ can be measured from the x- axis (Figure 2). Let ξ_{xy} be the shear strain rate in the Cartesian coordinates. It is evident that $\xi_{xy} = \xi_{\alpha\beta}$ at some point P if $\phi = 0$ at that point. By definition,

$$\xi_{xy} = \frac{1}{2}\left(\frac{\partial u_x}{\partial y} + \frac{\partial u_y}{\partial x}\right) \tag{6}$$

where u_x and u_y are the Cartesian components of velocity. It is seen from the geometry of Figure 2 that:

$$u_x = u_\alpha \cos\phi - u_\beta \sin\phi, \quad u_y = u_\alpha \sin\phi + u_\beta \cos\phi \tag{7}$$

where u_α and u_β are the velocity components referred to the $\alpha-$ and $\beta-$ lines, respectively. It is evident that:

$$\frac{\partial}{\partial x} = \frac{\partial}{R\partial\alpha}, \quad \frac{\partial}{\partial y} = -\frac{\partial}{S\partial\beta} \tag{8}$$

at P if $\phi = 0$. Substituting equation (7) into equation (6) and using equation (8) give ξ_{xy} at this point. Then, equation (5) yields:

$$\xi_{eq} = \frac{1}{\sqrt{3}}\left|-\frac{\partial u_\alpha}{S\partial\beta} + \frac{u_\beta}{S} + \frac{u_\alpha}{R} + \frac{\partial u_\beta}{R\partial\alpha}\right|. \tag{9}$$

The expansion (1) is valid in the vicinity of an envelope of characteristics where $S = 0$ or $R = 0$. Consider the case $R = 0$. In the vicintity of a generic point Q of such an envelope equation (9) becomes:

$$\xi_{eq} = \frac{1}{\sqrt{3}\left|R\right|}\left|\frac{\partial u_\beta}{\partial\alpha} + u_\alpha\right| \tag{10}$$

to leading order. Here the derivative $\partial u_\beta/\partial\alpha$ and the velocity component u_α are understood to be calculated at Q. Comparing equations (1) and (10) shows that:

$$R = R_0\sqrt{s} + o\left(\sqrt{s}\right) \tag{11}$$

as $s \to 0$. The tangent to the envelope under consideration coincides with the tangent to a $\beta-$ line at Q. Therefore, equation $(8)^1$ is valid with $s = mx$ where $m = \pm 1$. Substituting equation (11) into equation $(8)^1$ gives:

$$\frac{\partial R}{\partial \alpha} = \frac{R_0^2}{2m} + o(1) \tag{12}$$

as $s \to 0$. Integrating equation (12) yields:

$$R = \frac{R_0^2}{2m}\left(\alpha - \alpha_Q\right) + o\left(\alpha - \alpha_Q\right) \tag{13}$$

as $\alpha \to \alpha_Q$. Here α_Q is the value of α at Q. Substituting equation (11) into equation (10) and comparing the resulting expression with equation (1) show that:

$$D = \frac{1}{\sqrt{3}\left|R_0\right|}\left|\frac{\partial u_\beta}{\partial \alpha} + u_\alpha\right|. \tag{14}$$

The dependence of u_α, u_β and R on α and β is supposed to be known from the solution to a boundary value problem found by the method of characteristics. Therefore, the right hand side of equation (14) can be determined using the asymptotic expansion (13). Then, the strain rate intensity factor is readily found from equation (14). The case $S = 0$ can be treated in a similar manner.

3 VERIFICATION OF EQUATION (14)

Equation (14) can be verified by using an analytic solution. As an example, the solution found in [19] is used in the present paper. The boundary value problem consists of a planar deformation comprising the simultaneous shearing and expansion of a hollow cylinder. The solution has been given in cylindrical polar coordinates $(r\theta z)$ under the assumption that it is independent of θ and z. In particular, the radial and circumferential velocities are:

$$u_r = \frac{Ua}{r}, \quad u_\theta = \frac{Ur}{a}\left(\frac{\sqrt{b^4 - a^4}}{b^2} - \frac{\sqrt{r^4 - a^4}}{r^2}\right). \tag{15}$$

Here a is the internal radius, b is the external radius and U is the rate of expansion of the internal radius. The máximum friction law is supposed at $r = a$. The non-zero strain rate components in the cylindrical coordinates are determined from equation (15) as:

$$\xi_{rr} = -\frac{Ua}{r^2}, \quad \xi_{\theta\theta} = \frac{Ua}{r^2}, \quad \xi_{r\theta} = -\frac{Ua^3}{r^2\sqrt{r^4 - a^4}}.$$

Substituting these strain rates into equation (2) in which $q_1 \equiv r$ and $q_2 \equiv \theta$ yields:

$$\xi_{eq} = \frac{U}{\sqrt{3a}\sqrt{r-a}} + o\left(\frac{1}{\sqrt{r-a}}\right) \tag{16}$$

as $r \to a$. Since $s = r - a$ in the case under consideration, it follows from equations (1) and (16) that:

$$D = \frac{U}{\sqrt{3a}}. \tag{17}$$

The stress solution is given by [19]:

$$\sigma_{rr} - \sigma_{\theta\theta} = 2k\cos 2\psi, \quad \sigma_{r\theta} = k\sin 2\psi \tag{18}$$

where σ_{rr}, $\sigma_{\theta\theta}$ and $\sigma_{r\theta}$ are the components of the stress tensor in the cylindrical coordinates, $\pi/4 \le \psi \le \pi/2$ and

$$\frac{r}{a} = \frac{1}{\sqrt{\sin 2\psi}}. \tag{19}$$

It is seen from this equation that $\psi = \pi/4$ at the maximum friction surface. Using equation (18) the slope φ of the principal stress axis corresponding to σ_1 with respect to the *r*- axis is determined as:

$$\varphi = \psi . \tag{20}$$

Therefore, the slope of the $\alpha-$ lines is $\varphi - \pi/4$ and the slope of the $\beta-$ lines is $\varphi + \pi/4$ (Figure 1). The equations for the $\alpha-$ and $\beta-$ lines are:

$$\frac{rd\theta}{dr} = \tan\left(\varphi - \frac{\pi}{4}\right) \quad \text{and} \quad \frac{rd\theta}{dr} = \tan\left(\varphi + \frac{\pi}{4}\right), \tag{21}$$

respectively. Using equation (19) it is posible to replace differentition with respect to *r* with differentation with respect to ψ in equations (21). Then, these equations become:

$$-\tan\left(\psi - \frac{\pi}{4}\right)\cot 2\psi\, d\psi = d\theta \quad \text{and} \quad -\tan\left(\psi + \frac{\pi}{4}\right)\cot 2\psi\, d\psi = d\theta . \tag{22}$$

Let $r = r_\alpha(\theta)$ be the solution to equation (21)[1]. According to the convention accepted in [18] the radius of curvature of the $\alpha-$ lines is not negative in the problem under consideration. Therefore, this radius is given by:

$$R = \frac{\left[r_\alpha^2 + \left(dr_\alpha/d\theta\right)^2\right]^{3/2}}{\left|r_\alpha^2 + 2\left(dr_\alpha/d\theta\right)^2 - r_\alpha\, d^2 r_\alpha/d\theta^2\right|}. \tag{23}$$

It follows from equations (19), (20) and (21) that:

$$\frac{dr_\alpha}{d\theta} = \frac{a\cot\left(\psi - \pi/4\right)}{\sqrt{\sin 2\psi}} . \tag{24}$$

Then,

$$\frac{d^2 r_\alpha}{d\theta^2} = -\frac{a\left(1+\cos 4\psi - 4\sin 2\psi\right)\tan\left(\psi+\pi/4\right)}{2\cos 2\psi\left(1-\sin 2\psi\right)\sqrt{\sin 2\psi}}\,. \tag{25}$$

Here equation (22)[1] has been used. It follows from equation (24) that:

$$\frac{dr_\alpha}{d\theta} = \frac{a}{\left(\psi-\pi/4\right)} + O\left(\psi-\pi/4\right) \tag{26}$$

as $\psi \to \pi/4$ (or $r \to a$) and from equation (25) that:

$$\frac{d^2 r_\alpha}{d\theta^2} = -\frac{a}{2\left(\psi-\pi/4\right)^4} + O\left[\frac{1}{\left(\psi-\pi/4\right)^2}\right] \tag{27}$$

as $\psi \to \pi/4$. Substituting equations (26) and (27) into equation (23) yields:

$$R = a\left(\psi-\frac{\pi}{4}\right) + o\left(\psi-\frac{\pi}{4}\right) \tag{28}$$

as $\psi \to \pi/4$. Equation (19) is represented as:

$$r - a = a\left(\psi-\frac{\pi}{4}\right)^2 + o\left[\left(\psi-\frac{\pi}{4}\right)^2\right] \tag{29}$$

as $\psi \to \pi/4$. It follows from equations (28) and (29) that:

$$R = 2\sqrt{a}\sqrt{r-a} + o\left(\sqrt{r-a}\right) \tag{30}$$

as $r \to a$. Comparing equations (11) and (30) shows that:

$$R_0 = 2\sqrt{a}. \tag{31}$$

From the geometry of Figure 1 it is posible to find that:

$$\begin{aligned}
u_\alpha &= u_r\cos\left(\varphi-\frac{\pi}{4}\right) + u_\theta\sin\left(\varphi-\frac{\pi}{4}\right),\\
u_\beta &= u_r\cos\left(\varphi+\frac{\pi}{4}\right) + u_\theta\sin\left(\varphi+\frac{\pi}{4}\right),\\
\phi &= \theta+\varphi-\frac{\pi}{4},\\
\frac{\partial}{R\partial\alpha} &= \cos\left(\phi-\theta\right)\frac{\partial}{\partial r} + \frac{\sin\left(\phi-\theta\right)}{r}\frac{\partial}{\partial\theta}.
\end{aligned} \tag{32}$$

Eliminating φ in first three equations of this system by means of equation (20) yields:

$$u_\alpha = u_r \cos\left(\psi - \frac{\pi}{4}\right) + u_\theta \sin\left(\psi - \frac{\pi}{4}\right),$$
$$u_\beta = u_r \cos\left(\psi + \frac{\pi}{4}\right) + u_\theta \sin\left(\psi + \frac{\pi}{4}\right), \tag{33}$$
$$\phi = \theta + \psi - \frac{\pi}{4}.$$

Using equation (33)[3] equation (32)[4] can be transformed to:

$$\frac{\partial}{R\partial\alpha} = \cos\left(\psi - \frac{\pi}{4}\right)\frac{\partial}{\partial r} + \sin\left(\psi - \frac{\pi}{4}\right)\frac{\partial}{r\partial\theta}. \tag{34}$$

Since the solution is independent of θ equation (34) results in:

$$\frac{\partial u_\beta}{R\partial\alpha} = \cos\left(\psi - \frac{\pi}{4}\right)\frac{\partial u_\beta}{\partial r}. \tag{35}$$

Differentiating equation (33)[2] with respect to *r* gives:

$$\frac{\partial u_\beta}{\partial r} = \frac{\partial u_r}{\partial r}\cos\left(\psi + \frac{\pi}{4}\right) - u_r \sin\left(\psi + \frac{\pi}{4}\right)\frac{\partial \psi}{\partial r} + \frac{\partial u_\theta}{\partial r}\sin\left(\psi + \frac{\pi}{4}\right) + u_\theta \cos\left(\psi + \frac{\pi}{4}\right)\frac{\partial \psi}{\partial r}. \tag{36}$$

Differentiating equations (15) and (19) yields:

$$\frac{\partial u_\theta}{\partial r} = \frac{U}{a}\left[\frac{\sqrt{b^4 - a^4}}{b^2} - \frac{\left(a^4 + r^4\right)}{r^2\sqrt{r^4 - a^4}}\right],$$
$$\frac{\partial \psi}{\partial r} = -\frac{a^2}{r^3 \cos 2\psi}. \tag{37}$$

It follows from these equations and (29) that:

$$\frac{\partial u_\theta}{\partial r} = -\frac{U}{a\left(\psi - \pi/4\right)} + o\left(\psi - \frac{\pi}{4}\right),$$
$$\frac{\partial \psi}{\partial r} = \frac{1}{2a\left(\psi - \pi/4\right)} + o\left(\psi - \frac{\pi}{4}\right). \tag{38}$$

as $\psi \to \pi/4$. Substituting equations (15) and (38) into equaton (36) gives:

$$\frac{\partial u_\beta}{\partial r} = -\frac{3U}{2a\left(\psi - \pi/4\right)} + o\left(\psi - \pi/4\right) \tag{39}$$

as $\psi \to \pi/4$. It follows from equations (28), (35) and (39) that:

$$\frac{\partial u_\beta}{\partial \alpha} = -3U + o(1) \tag{40}$$

as $\psi \to \pi/4$. It is evident that $u_\alpha = U$ at $r = a$. Substituting this value of u_α, (31) and (40) into (14) shows that the strain rate intensity factor found by means of this equation coincides with that given by (17).

4 COMPRESSION OF A PLASTIC LAYER BETWEEN PARALLEL PLATES

A schematic diagram of the process is shown in Figure 3. A layer of plastic material is compressed between rigid parallel plates. The current thickness of the layer is denoted by $2h$ and current width by $2w$. The velocity of each plate is V. The maximum friction law is assumed at $y = \pm h$. This problem is known as Prandtl's problem [18]. The Prandtl's cycloid solution to this problem can be found in any textbook and monograph on plasticity theory (see, for example, [18]). It follows from this approximate solution that [20]:

$$D = \sqrt{\frac{2}{3}} \frac{V}{\sqrt{h}}. \tag{41}$$

A numerical solution to the problem under consideration has been proposed in [21]. This solution has been reproduced in the present paper and then complemented with a procedure to calculate the strain rate intensity factor by means of equation (14). The distibution of the dimensionless strain rate intensity factor d defined as $d = D\sqrt{h}/V$ along the friction surface is depicted in Figure 4 at $w/h = 13$. The broken line corresponds to equation (41). It is seen from Figure 4 that even though an average value of the strain rate intensity factor for a finite layer approaches the value given by Prandtl's solution, local values of the strain rate intensity factor for the finite layer may be significantly different from that given by (41).

5 CONCLUSIONS

- The strain rate intensity factor for rigid perfectly plastic material under plane strain conditions has been derived in characteristic coordinates.
- The expression for the strain rate intensity factor in characteristic coordinates has been implemented into a numerical code based on the method of characteristics.
- The strain rate intensity factor has been calculated for compression of a rigid plastic layer of finite width. It has been shown that local values of the strain rate intensity factor for a layer of finite width may be significantly different from that found from the solution for an infinite layer even though the ratio of the width to thickness is quite large.
- The distribution of the strain rate intensity factor along the friction surface is discontinuous (Figure 4).

Acknowledgment – This research was made posible by grants RNF-14-11-00844 and NSH-1275.2014.1.

REFERENCES

[1] Alexandrov, S. and Richmond, O. Singular Plastic Flow Fields Near Surfaces of Maximum Friction Stress. *Int. J. Non-Linear Mech.* (2001) **36**:1-11.

[2] Ng, E.-G., Aspinwall, D.K., Brazil, D. and Monaghan, J. Modelling of Temperature and Forces When Orthogonally Machining Hardened Steel. *Int. J. Mach. Tool Manuf.* (1999) **39**:885-903.

[3] Yigit, K. and Tugrul, O. Predictive Analytical and Thermal Modeling of Orthogonal

Cutting Process—Part I: Predictions of Tool Forces, Stresses, and Temperature Distributions. *ASME J. Manuf. Sci. Technol.* (2006) **128**:435-444.
[4] Ramesh, E.-G. and Melkote, S.N. Modeling of White Layer Formation Under Thermally Dominate Condition in Orthogonal Machining of Hardened AISI 52100 Steel. *Int. J. Mach. Tool Manuf.* (2008) **48**:402-414.
[5] Lalwani, D.I., Mehta, N.K. and Jain, P.K. Extension of Oxley's Predictive Machining Theory for Johnson and Cook Flow Stress Model. *J. Mater. Process. Technol.* (2009) **209**:5305-5312.
[6] Akbar, F., Mativenga, P.T. and Sheikh, M.A. An Experimental and Coupled Thermo-Mechanical Finite Element Study of Heat Partition Effects in Machining. *Int. J. Adv. Manuf. Technol.* (2010) **46**:491-507.
[7] Molinari, A., Cheriguene, R. and Miguelez, H. Contact Variables and Thermal Effects at the Tool-chip Interface in Orthogonal Cutting. *Int. J. Solids Struct.* (2012) **49**:3774-3796.
[8] Chen, G., Li, J., He, Y. and Ren, C. A New Approach to the Determination of Plastic Flow Stress and Failure Initiation Strain for Aluminium Alloys Cutting Process. *Comp. Mater. Sci.* (2014) **95**:568-578.
[9] Agmell, M., Ahadi, A. and Stahl, J.-E. Identification of Plastic Constants from Orthogonal Cutting and Inverse Analysis. *Mech. Mater.* (2014) **77**:43-51.
[10] Kim, T.-K. and Ikeda, K. Flow Behavior of the Billet Surface Layer in Porthole Die Extrusion of Aluminium. *Metall. Mater. Trans.* (2000) **31A**:1635-1643.
[11] Wideroe, F. and Welo, T. Conditions for Sticking Friction Between Aluminium Alloy AA6060 and Tool Steel in Hot Forming. *Key Engng Mater.* (2012) **491**:121-128.
[12] Sanabria, V., Mueller, S., Gall, S. and Reimers, W. Investigation of Friction Boundary Conditions During Extrusion of Aluminium and Magnesium Alloys. *Key Engng Mater.* (2014) **611-612**:997-1004.
[13] Sanabria, V., Mueller, S. and Reimers, W. Microstructure Evolution of Friction Boundary Layer During Extrusion of AA 6060. *Proc. Engng* (2014) **81**:586-591.
[14] Lyamina, E. and Alexandrov, S. Application of the Strain Rate Intensity Factor to Modeling Material Behavior in the Vicinity of Frictional Interfaces, In: Trends in Computational Contact Mechanics, Series "Lecture Notes in Applied and Computational Mechanics", eds. Giorgio Zavarise and Peter Wriggers, Springer, Vol. 58, pp.291-320 (2011).
[15] Alexandrov, S. and Lyamina, E. Singular Solutions for Plane Plastic Flow of Pressure-Dependent Materials. *Dokl. Phys.* (2002) **47**:308-311.
[16] Alexandrov, S. and Jeng, Y.-R. Singular Rigid/Plastic Solutions in Anisotropic Plasticity Under Plane Strain Conditions. *Cont. Mech. Therm.* (2013) **25**:685-689.
[17] Alexandrov, S. and Mustafa, Y. Singular Solutions in Viscoplasticity Under Plane Strain Conditions. *Meccanica* (2013) **48**:2203-2208.
[18] Hill, R. *The mathematical theory of plasticity*. Clarendon Press, (1950).
[19] Alexandrov, S. and Harris, D. Comparison of Solution Behaviour for Three Models of Pressure-Dependent Plasticity: A Simple Analytical Example. *Meccanica* (2013) **48**:2203-2208.
[20] Alexandrov, S. The Strain Rate Intensity Factor and Its Applications: A Review. *Mater. Sci. Forum* (2009) **623**:1-20.
[21] Hill, R., Lee, E.H. and Tupper, S.J. A Method of Numerical Analysis of Plastic Flow

in Plane Strain and Its Application to the Compression of a Ductile Material Between Rough Plates. *Trans. ASME J. Appl. Mech.* (1951) **18**:46-52.

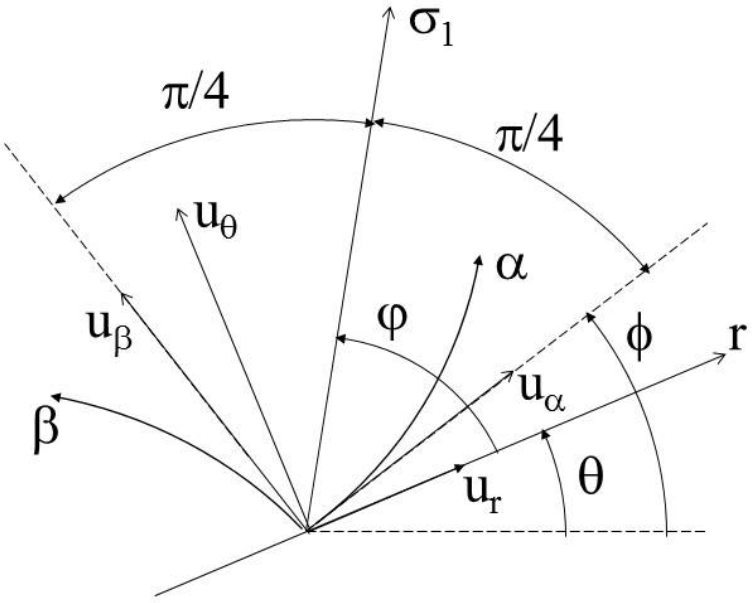

Figure 1: Characteristic and cylindrical coordinates

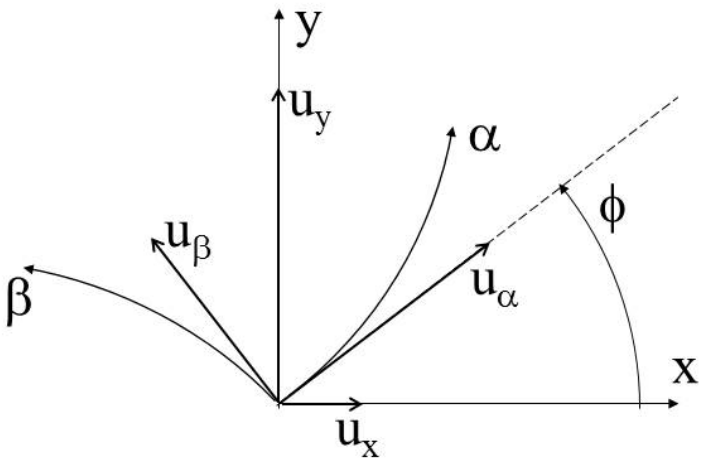

Figure 2: Characteristic and Cartesian coordinates

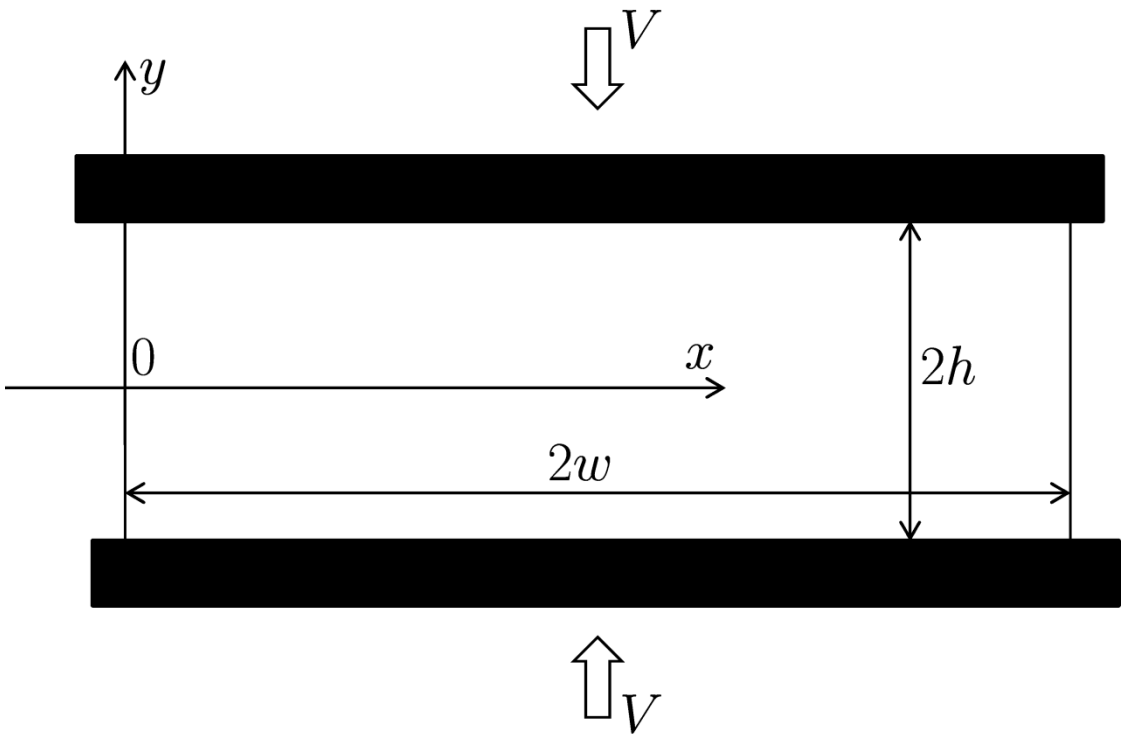

Figure 3: Compression of a plastic layer - notation

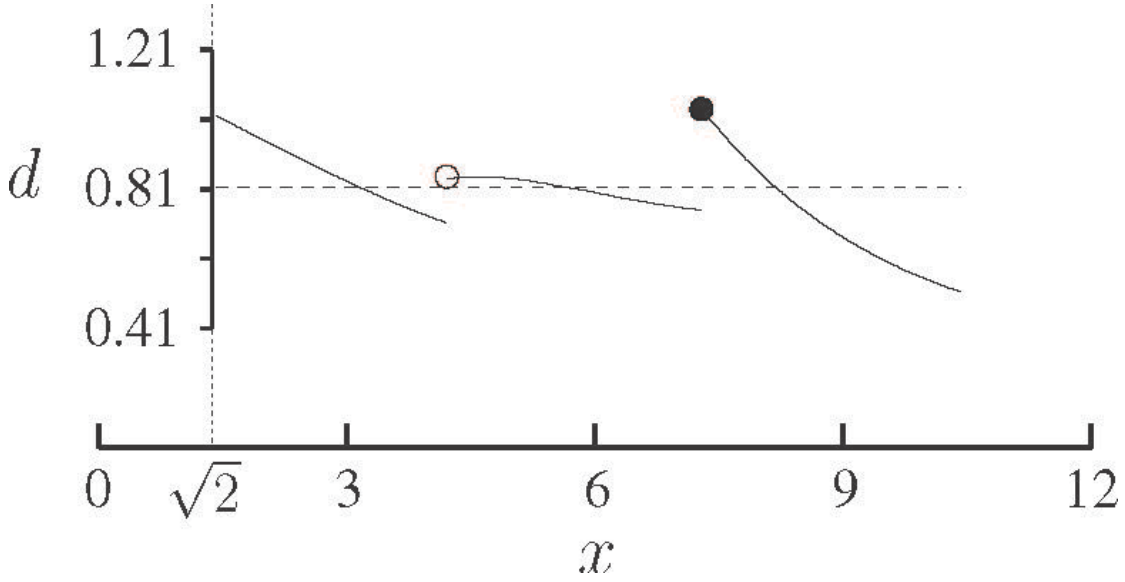

Figure 4: Distribution of the dimensionless strain rate intensity factor along the friction surface